A Hit-or-Miss Transform for Multivariate Images

Erchan Aptoula, Sébastien Lefèvre, Christian Ronse

A Hit-or-Miss Transform for Multivariate Images

E. Aptoula, S. Lefèvre*, C. Ronse

LSIIT UMR-7005 CNRS-ULP, Pôle API, Blvd Sébastien Brant, PO Box 10413, 67412 Illkirch Cedex, France

Abstract

The hit-or-miss transform (HMT) is considered to be among the fundamental operations in the morphological toolbox. Initially, it was defined for binary images, as a morphological approach to the problem of template matching, whereas its extension to grey-level data has been problematic, leading to multiple definitions, that have been only recently unified by means of a common theoretical foundation. In this paper, we generalise these definitions to the case of multivariate images, and propose a vectorial HMT, allowing the detection of objects over multiple image channels. Moreover, in order to counter the operator's extreme sensitivity to variations, rank order filters as well as synthetic structuring functions are studied in the context of multivariate data. We additionally present examples of the use of the suggested operator in combination with colour images.

Key words: Hit-or-miss transform, colour HMT, multivariate morphology, template matching.

1. Introduction

The *hit-or-miss transform* (HMT) is a powerful morphological tool that was among the initial morphological transforms developed by Matheron (1975) and Serra (1982). It constitutes the morphological approach to pattern matching. Its initial definition for binary images has been widely used since then, with the purpose of shape recognition (Bhattacharya et al., 1995; Bloomberg and Vincent, 2000), while multiple theoretical extensions have been proposed in order to improve its performance (Bloomberg and Vincent, 2000; Soille, 2002b; Zhao and Daut, 1991). The extension of this transform to grey-level images however has not been straightforward, since it is neither increasing nor decreasing, hence leading to multiple definitions, such as those of Ronse (1996), Soille (2002a)

*Corresponding author. Tel: +33 (0)3 90 24 45 70; fax: +33(0)3 90 24 44 55
Email address: lefevre@lsiit.u-strasbg.fr (S. Lefèvre)

and Barat et al. (2003). Only recently a unified theoretical framework has been proposed for grey-level HMTs by Naegel et al. (2007a).

As far as multivariate image data is concerned, the potential of the HMT has been left largely unexplored (Wilson, 1989), with the exception of the recent work from Weber and Lefèvre (2008), which presents a novel approach for a multivariate HMT based however on a marginal strategy. The reason of this situation, besides the aforementioned ambiguities of its extension to grey-level data, lies additionally in the complications inherent to the application of morphological operators to multivariate images. Specifically, a multivariate ordering is required, in order to impose a complete lattice structure on the vectorial data. Considering the numerous possibilities of multivariate ordering, an almost equal number of approaches to multivariate morphology has also been proposed, a recent survey of which is provided by Aptoula and Lefèvre (2007). Despite these difficulties, a vectorial HMT has an important potential, that can be exploited for instance with the purpose of object detection from multispectral remote sensing data, or colour object recognition in the context of content-based image retrieval (CBIR).

Motivated by this application potential, we propose a vectorial HMT (VHMT) definition, capable of detecting objects from colour images, based on colour templates. Its main advantage with respect to a marginal or component-wise definition, lies in its capacity to be further configured by means of the vector ordering choice, hence allowing the introduction of a priori information concerning the sought object's inter-channel presence. Furthermore, since the HMT is inherently sensitive to image variations, a couple of approaches aiming to counter this drawback, already used with binary and grey-level images (Barat et al., 2003; Doh et al., 2002; Soille, 2002b), are studied in the case of colour data. Specifically, rank order filters as well as "synthetic" structuring functions are discussed.

After presenting the case of binary and grey-level HMT in Sec. 2, the vectorial case is elaborated in Sec. 3, where the VHMT definition is given. Then Sec. 4 presents the adaptation to the vectorial case of two known techniques for increasing the robustness of the HMT.

2. Binary and grey-level HMT

In this section, we will review briefly the binary and grey-level approaches to the HMT. The initial binary definition of the HMT (Matheron, 1975; Serra, 1982), consists in searching in the input binary image $X \in \mathcal{P}(\mathcal{E})$, $\mathcal{E} = \mathbb{R}^d$ (d-dimensional Euclidean space) or $\mathbb{Z}^d$ (d-dimensional discrete space), a template described by a couple of structuring elements (SE), $A, B \in \mathcal{P}(\mathcal{E})$ (Fig. 1). Specifically, it attempts to match A *(foreground SE)* within the image (i. e. "*a hit*") while also matching B *(background SE)* in its background $X^c = \mathcal{E} \setminus X$ (i. e. "*a miss*"):

$$X \circledast (A, B) = (X \ominus A) \cap (X^c \ominus B) \tag{1}$$

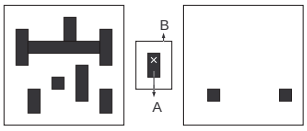

Figure 1: From left to right, the input binary image X (foreground in black, background in white), the sought template (A, B), and the output of Eq. (1). The "×" within A marks the center of the SE.

where $\ominus$ denotes the binary erosion operator, and it is assumed that $A \cap B = \emptyset$. However, since Eq. (1) uses both X and X^c, its extension to grey-level images has not been straightforward.

As a matter of fact, this extension was not realised until after the HMT was expressed in terms of an *interval operator* η, through the work of Heijmans and Serra (1992). For $A, B \in \mathcal{P}(\mathcal{E})$, $A \subseteq B$:

$$\eta_{[A,B]}(X) = \{p \in \mathcal{E} \mid A_p \subseteq X \subseteq B_p\} = X \circledast (A, B^c) \tag{2}$$

where $A_p = \{x + p \mid x \in A\}$ denotes the translate of A by p. Through this formulation, the grey-level HMT of Ronse (1996) and subsequently of Soille (2002a) have been defined, and along with others (Barat et al., 2003; Khosravi and Schaefer, 1996; Raducanu and Grana, 2000; Schaefer and Casasent, 1995), they have been recently unified into a common theoretical framework for grey-level interval operators (Naegel et al., 2007a).

More precisely, in the case of grey-level images, an image $F \in \mathcal{T}^{\mathcal{E}}$, ($\mathcal{T}$ being a complete lattice, usually $\overline{\mathbb{R}}$ or $\overline{\mathbb{Z}}$), besides a SE, can also interact with a structuring function (SF) $V \in \mathcal{T}^{\mathcal{E}}$. Consequently, the sought template is translated not only horizontally (by a point $p \in \mathcal{E}$), but vertically as well (by a finite grey-level $t \in \mathcal{T}$) (Fig. 2) in an attempt to detect the positions where it fits. Specifically, a translation by a couple (p, t) is $V_{(p,t)} : x \to V(x - p) + t$. According to the unified theory for grey-level HMT (Naegel et al., 2007a), such an operator is decomposed into two stages:

- the *fitting*, where the locations fitting the given structuring functions, describing the sought template, are computed,
- and *valuation*, where the resulting image containing the previously detected locations is constructed.

To explain, there are two types of fittings. Given a grey-level image F, along with a couple of structuring functions V, W, $(V \leq W)$ describing the sought template, there is first:

$$H_{V,W}(F) = \left\{(p, t) \in \mathcal{E} \times \mathcal{T} \mid V_{(p,t)} \leq F \leq W_{(p,t)}\right\} \tag{3}$$

the inequality of which according to Naegel et al. (2007a) is equivalent to:

$$\varepsilon_V(F)(p) \leq t \leq \delta_{W^*}(F)(p) \tag{4}$$

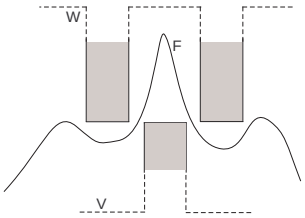

Figure 2: The integral interval operator, Eq. (9).

where $W^* : x \to -W(-x)$, is the *dual* of W and ε, δ represent respectively the grey-level erosion and dilation with a SF:

$$\varepsilon_B(F)(p) = \inf_{x \in \mathrm{supp}(B)} \{F(p+x) - B(x)\} \quad (5)$$

$$\delta_B(F)(p) = \sup_{x \in \mathrm{supp}(B)} \{F(p-x) + B(x)\} \quad (6)$$

where $\mathrm{supp}(B) = \{p \in \mathcal{E} \mid B(p) > \bot\}$, while inf and sup denote respectively the infimum and supremum.

The other fitting is:

$$K_{V,W}(F) = \left\{(p,t) \in \mathcal{E} \times \mathcal{T} \mid V_{(p,t)} \leq F \ll W_{(p,t)}\right\} \quad (7)$$

where $F \ll W$ means that there is some $h > 0$ such that for every $p \in \mathcal{E}$ we have $F(p) \leq W(p) - h$. Besides, the inequality of the second fitting once more according to Naegel et al. (2007a) is equivalent to:

$$\varepsilon_V(F)(p) \leq t < \delta_{W^*}(F)(p) \quad (8)$$

Likewise, there are two [1] types of valuations. First there is *supremal* valuation, which for every point p of fit couple (p,t), takes the supremum of t, and then there is *integral* valuation which instead for every point p of fit couple (p,t), uses the length of the interval of t for which the couples (p,t) fit. Moreover, Soille's grey-level HMT (Soille, 2002a) employs the fitting K of Eq. (7) along with an integral valuation, which leads to the *integral interval operator* η^I (Fig. 2):

$$\eta^I_{[V,W]}(F)(p) = \max\{\varepsilon_V(F)(p) - \delta_{W^*}(F)(p), 0\} \quad (9)$$

It should be noted that the reason for choosing the fitting K instead of H is that it produces a semi-open interval $[\varepsilon_V(F)(p), \delta_{W^*}(F)(p)[$ and not a closed one. Thus in the discrete case the interval length formulation corresponds indeed to that of Eq. (9). Ronse's grey-level HMT on the other hand, uses the fitting

[1] In fact there is also the *binary* valuation, which consists in taking the set of points $p \in \mathcal{E}$ for which there is at least one $t \in \mathcal{T}$ such that (p,t) fits.

H of Eq. (3) combined with a supremal valuation, which leads to the *supremal interval operator* η^S:

$$\eta^S_{[V,W]}(F)(p) = \begin{cases} \varepsilon_V(F)(p) & \text{if } \varepsilon_V(F)(p) \geq \delta_{W^*}(F)(p), \\ \bot & \text{otherwise} \end{cases} \tag{10}$$

where $\bot$ is the least element of $\mathcal{T}$, $-\infty$ if $\mathcal{T} = \overline{\mathbb{R}}$. In the next section, the grey-level integral operators of Eqs. (9) and (10) will be extended to multivariate images.

3. Vectorial HMT

Given Eqs. (9) and (10) in combination with multivariate image data, the obvious way of searching for a multivariate template would be to apply them independently to each image channel. This principle is endorsed by Wilson (1989), where binary multivariate images are considered. A more original approach using channel specific thresholds is presented by Weber and Lefèvre (2008), which however is still based on a marginal strategy. In short, these approaches ignore any eventual correlation among image channels. This drawback can be solved using a (possibly costly) decorrelation method (e.g. PCA) and applying the marginal strategy on decorrelated channels. However this solution does not ensure to preserve input vectors, which may be a serious drawback in some applications. Thus the alternative consists in defining multivariate morphological operators (Aptoula and Lefèvre, 2007).

In the multivariate case, the pixel values of images are now in $\mathcal{T} = \overline{\mathbb{R}}^n$ or $\overline{\mathbb{Z}}^n, n > 1$. The initial step consists in defining the erosion and dilation operators for multivariate images in combination with multivariate SF. More precisely, these operators are once more based on horizontal translations (by a point $p \in \mathcal{E}$) as well as on vertical ones (by a finite pixel value $\mathbf{t} \in \mathcal{T}$) as in the grey-level case, the difference is however that pixel values are now multidimensional; in particular, given a multivariate image $\mathbf{F} : \mathcal{E} \to \mathcal{T}$:

$$\forall\, (p, \mathbf{t}) \in \mathcal{E} \times \mathcal{T},\ \ \mathbf{F}_{(p,\mathbf{t})}(x) = \mathbf{F}(p - x) + \mathbf{t} \tag{11}$$

Furthermore, according to the fundamental works of Heijmans and Ronse (Heijmans, 1994; Heijmans and Ronse, 1990), translations need to be complete lattice automorphisms (i. e. bijections $\mathcal{T} \to \mathcal{T}$ that preserve order, and whose inverse also preserve order). Consequently, the vector ordering ($\leq_v$) from which the complete lattice is derived, must be translation invariant. In other words:

$$\forall\, \mathbf{w}, \mathbf{w}', \mathbf{t} \in \mathcal{T},\ \ \mathbf{w} \leq_v \mathbf{w}' \Leftrightarrow \mathbf{w} + \mathbf{t} \leq_v \mathbf{w}' + \mathbf{t} \tag{12}$$

Thus we can give the definition of the erosion and dilation respectively of a multivariate image $\mathbf{F}$ by a multivariate SF $\mathbf{B}$ as a simple extension of Eqs. (5) and (6):

$$\boldsymbol{\varepsilon}_{\mathbf{B}}(\mathbf{F})(p) = \inf_{\substack{v \\ x \in \mathrm{supp}(\mathbf{B})}} \{\mathbf{F}(p + x) - \mathbf{B}(x)\} \tag{13}$$

$$\boldsymbol{\delta}_{\mathbf{B}}(\mathbf{F})(p) = \sup_{\substack{v \\ x \in \mathrm{supp}(\mathbf{B})}} \{\mathbf{F}(p - x) + \mathbf{B}(x)\} \tag{14}$$

where here $\inf_v$ and $\sup_v$ denote respectively the infimum and supremum based on the vector ordering ($\leq_v$) under consideration. Hence, these formulations form an adjunction as demanded by (Heijmans, 1994; Heijmans and Ronse, 1990) and besides, with a flat SE (i. e. $\forall\, x,\ \mathbf{B}(x) = \mathbf{0}$) they are reduced to the flat multivariate erosion and dilation formulations. Furthermore, thanks to Eq. (12), both fitting equivalences between Eqs. (3) and (4) as well as between Eqs. (7) and (8) become directly extendable to this case by replacing the grey-level operators with their multivariate counterparts. As to valuation, the same options as before are available, however the supremum is of course now computed among vectors through the vector ordering in use. In the case of integral valuation, a vector distance now can be used in order to measure the distance among the vectors that have fit. Consequently one can express the multivariate versions of the integral and supremal interval operators respectively as follows:

$$\boldsymbol{\eta}^I_{[\mathbf{V},\mathbf{W}]}(\mathbf{F})(p) = \begin{cases} \|\boldsymbol{\varepsilon}_{\mathbf{V}}(\mathbf{F})(p) - \boldsymbol{\delta}_{\mathbf{W}^*}(\mathbf{F})(p))\| & \text{if } \boldsymbol{\varepsilon}_{\mathbf{V}}(\mathbf{F})(p) >_v \boldsymbol{\delta}_{\mathbf{W}^*}(\mathbf{F})(p) \\ 0 & \text{otherwise.} \end{cases} \tag{15}$$

$$\boldsymbol{\eta}^S_{[\mathbf{V},\mathbf{W}]}(\mathbf{F})(p) = \begin{cases} \boldsymbol{\varepsilon}_{\mathbf{V}}(\mathbf{F})(p) & \text{if } \boldsymbol{\varepsilon}_{\mathbf{V}}(\mathbf{F})(p) \geq_v \boldsymbol{\delta}_{\mathbf{W}^*}(\mathbf{F})(p) \\ \bot & \text{otherwise.} \end{cases} \tag{16}$$

where $\mathbf{V} \leq_v \mathbf{W}$. As far as $\boldsymbol{\eta}^I$ is concerned, it provides a non-zero output at positions p where $\mathbf{V}_{(p,\mathbf{t})} \leq_v \mathbf{F} \ll_v \mathbf{W}_{(p,\mathbf{t})}$ for some $\mathbf{t} \in \mathcal{T}$ according to the ordering in use. It should also be noted that the grey-level valuation choice by means of the Euclidean norm ($\|\cdot\|$) is arbitrary, and a multi-dimensional valuation is of course possible. As to $\boldsymbol{\eta}^S$, it produces a non-zero output at positions p where $\mathbf{V}_{(p,\mathbf{t})} \leq_v \mathbf{F} \leq_v \mathbf{W}_{(p,\mathbf{t})}$ for some $\mathbf{t} \in \mathcal{T}$. The choice between $\boldsymbol{\eta}^I$ and $\boldsymbol{\eta}^S$ depends on the application under consideration. The first one measures the interval of possible positions and thus can be used to determine how much an object or image fits a given pattern. The second one returns the erosion value (i.e. the highest possible position) and thus can be used in a filtering purpose to build an idempotent pseudo-opening defined as $\boldsymbol{\delta}_{\mathbf{V}}(\boldsymbol{\eta}^S_{[\mathbf{V},\mathbf{W}]}(\mathbf{F}))$, see (Ronse, 1996; Naegel et al., 2007a) for more details.

Therefore, the only obstacle preventing the definition of a VHMT is a translation preserving vector ordering. This useful property, among others, is provided by the standard *lexicographical ordering* frequently employed in the context of multivariate morphology since it provides a total ordering and enable to define priority among the different channels (Aptoula and Lefèvre, 2007):

$$\forall\, \mathbf{v}, \mathbf{v}' \in \mathbb{R}^n,\ \ \mathbf{v} <_L \mathbf{v}' \Leftrightarrow \exists\, i \in \{1, \ldots, n\},\ \ (\forall\, j < i,\ v_j = v'_j) \wedge (v_i < v'_i) \tag{17}$$

while for instance its recent variation α-modulus lexicographical (Angulo, 2005), does not provide it. Moreover, the chosen ordering directly affects the behaviour of VHMT. For instance, in the case of lexicographical ordering, which is known for its tendency of prioritising the first vector component, this property can be

observed in the detection process of VHMT. In particular, during the fitting stage where the erosion and dilation outputs are computed, since it is the first vector component that decides the outcome of the majority of lexicographical comparisons, fitting the first channel of the vectorial structuring function becomes more important with respect to the rest. This example is illustrated in Fig. 3, where although only $V_1 \leq F_1$, according to the lexicographical ordering, $\mathbf{V} <_L \mathbf{F}$. This property would allow for a prioritised detection, where a colour template might be searched for example with more emphasis on some components than others (e.g. brightness rather than saturation (Angulo, 2005)).

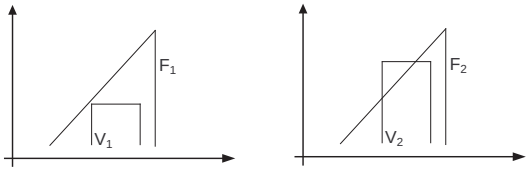

Figure 3: A two-channel image $\mathbf{F} = (F_1, F_2)$ and a vectorial structuring function $\mathbf{V} = (V_1, V_2)$.

A more practical example of VHMT is given in Fig. 4, where the yellow sign of the middle is sought using a lexicographical (pre-)ordering in the LSH space (Angulo, 2005) where saturation (S) is compared after luminance (L), and hue does not participate in comparisons due to its periodicity. More precisely, the SF positioned under the object ($\mathbf{V}$) is formed by decreasing the pixel values of the template by a fixed amount (e. g. 3, if pixel values are in $[0, 255]$), whereas the background SF ($\mathbf{W}$) is formed by increasing it. Hence, the operator looks for all objects that fit between the upper and lower SF based on the lexicographical principle. In this particular case, as the hue is not taken into account, it detects the left sign despite its different hue value, while it misses the right sign, even though its only difference from the template are a few white points; a result that asserts the sensitivity of the operator.

4. Strategies for robust VHMT

As the HMT attempts to perform an exact match of the given pattern, it becomes sensitive to noise, occlusions, and even to the slightest variations of the shape of the object to detect. Consequently a series of approaches have been implemented for the binary and grey-level versions of the operator, with the purpose of countering this drawback and increasing its practical interest. Among others, rank order filters (Ronse, 1996; Soille, 2002b) and "synthetic" SE (Barat et al., 2003; Doh et al., 2002) can be mentioned. This section concentrates on these two methods and studies their use in the case of multivariate images in combination with VHMT.

Another feature to take into account when considering practical applications is the computational complexity. It is not specific to the proposed definition but

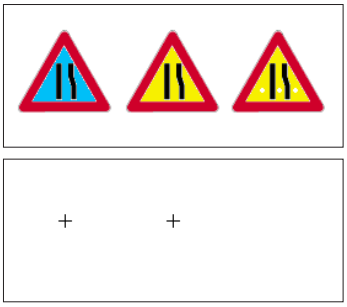

Figure 4: In the first row are three images, of which the middle is the sought pattern. The second row shows the locations where it was detected by Eq. (15) based on a lexicographical ordering of luminance and saturation.

is rather related to both the standard HMT definition and the vector ordering into consideration. The reader will find in (Naegel et al., 2007b) and (Aptoula and Lefèvre, 2007) some comments on these respective issues.

4.1. Rank order based VHMT

A rank order filter of k^{th} rank is a transformation, where given a grey-level image F and a SE B, the result becomes:

$$(F\square_k B)(p) = k^{th} \text{ largest of } F(p+x),\ x \in B \tag{18}$$

with $k \in \{1, \ldots, |B|\}$. Obviously, $F\square_1 \check{B}$ and $F\square_{|B|}B$ with $\check{B} = \{-x | x \in B\}$ the reflection of B, correspond respectively to the dilation and erosion of F by B. Moreover, always in the context of grey-level data, a rank order filter of k^{th} rank, is equivalent to the supremum of erosions using all possible SE with k points, and respectively to the infimum of dilations using all possible SE with $|B| - k + 1$ points (Soille, 2002a). Due to this property, the binary HMT of Eq. (1) has been reformulated in the literature, by replacing the erosion in its expression with a rank order filter of rank $k < |B|$, hence making it possible to detect binary templates even in conditions of partial occlusion.

In order to achieve the same additional robustness in the case of a multivariate image $\mathbf{F}$ along with a multivariate SF $\mathbf{B}$ and a vector ordering $\leq_v$, one can redefine the rank order filter of k^{th} rank as follows:

$$\zeta^k_{\mathbf{B}}(\mathbf{F})(p) = k^{th} \text{ largest of } \mathbf{F}(p+x) - \mathbf{B}(x),\ x \in \text{supp}(\mathbf{B}) \tag{19}$$

$$\theta^k_{\mathbf{B}}(\mathbf{F})(p) = k^{th} \text{ largest of } \mathbf{F}(p-x) + \mathbf{B}(x),\ x \in \text{supp}(\mathbf{B}) \tag{20}$$

where $k \in \{1, \ldots, |\,\text{supp}(\mathbf{B})|\}$. Naturally, the vectors are sorted using $\leq_v$. Thus, $\boldsymbol{\varepsilon}_{\mathbf{B}} = \zeta^{|\,\text{supp}(\mathbf{B})|}_{\mathbf{B}}$ and $\boldsymbol{\delta}_{\mathbf{B}} = \theta^1_{\mathbf{B}}$. Consequently, we can now formulate a rank-based VHMT, following the definition given by Soille (2003) for grey-level images, capable of detecting the sought template $(\mathbf{V}, \mathbf{W})$ even if m and n pixels do not match respectively the foreground and the background:

$$\boldsymbol{\eta}^I_{[\mathbf{V},\mathbf{W}],m,n}(\mathbf{F})(p) = \begin{cases} \|\zeta^m_{\mathbf{V}}(\mathbf{F})(p) - \theta^n_{\mathbf{W}^*}(\mathbf{F})(p))\| & \text{if } \zeta^m_{\mathbf{V}}(\mathbf{F})(p) >_v \theta^n_{\mathbf{W}^*}(\mathbf{F})(p) \\ 0 & \text{otherwise.} \end{cases} \tag{21}$$

where $m \in \{1, \ldots, |\operatorname{supp}(V)|\}$ and $n \in \{1, \ldots, |\operatorname{supp}(W)|\}$. It should also be noted that $\boldsymbol{\eta}^I_{[\mathbf{V},\mathbf{W}],|\operatorname{supp}(V)|,1} = \boldsymbol{\eta}^I_{[\mathbf{V},\mathbf{W}]}$. Fig. 5 contains an example of the result given by this operator, where the leftmost image is sought under the same conditions as in Fig. 4. However, this time even though the right example has a red/brown stripe, it is still succesfully detected. This is due to the use of the 750^{th} rank, a number equal to the amount of different pixels between the two images. Thus the rank based operator can allow a flexibility margin large enough to realise the detection in case of pixel value variations, due to reasons such as noise.

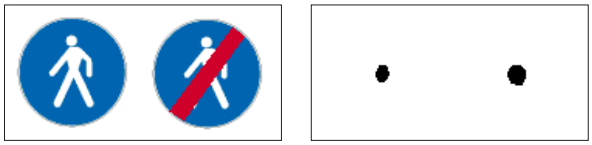

Figure 5: On the left is a couple of images, of which the leftmost is the sought pattern, and on the right is the output of $\boldsymbol{\eta}^I_{[\mathbf{V},\mathbf{W}],750,750}$, Eq. (21).

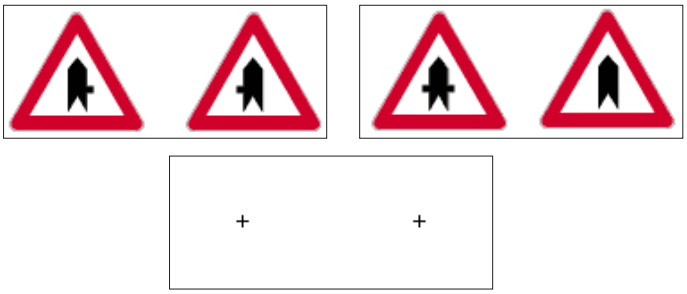

Figure 6: In the first row, from left to right the two images to detect, and the corresponding lower and upper synthetic SF computed through Eqs. (22) and (23); the second row contains the result of VHMT, Eq. (15).

4.2. Synthetic structuring functions

Although multivariate rank order filters make it possible to detect partial matches, Eq. (21) still hardly satisfies practical needs, since the objects corresponding to the sought template may vary considerably. Consider for instance

the case illustrated in Fig. 6 (top-left). This situation is of course present in the context of detection from grey-level images as well. One way of countering it, as explained in (Barat et al., 2003; Doh et al., 2002), is to employ a set of example images, from which a common "synthetic" template is formed.

More precisely, the foreground is represented by the minimum and the background by the maximum of the given set of examples ($\{\mathbf{V}_i\}, \{\mathbf{W}_j\}$). Thus, in the multivariate case the same technique may be employed merely by using the chosen vector ordering $\leq_v$:

$$\mathbf{V}(x) = \inf_i{}_v \{\mathbf{V}_i(x)\} \quad (22)$$

$$\mathbf{W}(x) = \sup_j{}_v \{\mathbf{W}_j(x)\} \quad (23)$$

Returning to Fig. 6, it suffices to compute the templates corresponding to the images at the top-left by means of this operation, and the VHMT of Eq. (15) detects both successfully.

5. Conclusion

A vectorial HMT definition is proposed, which allows for the use of vectorial structuring functions, making it possible to detect multivariate templates within multivariate data such as colour images. The additional parameter of choosing a vector ordering, opens up new combination possibilities, allowing to refine the detection properties of the resulting operator. Furthermore, two classical techniques for enhancing the flexibility of HMT have been studied in combination with multivariate images. Future work will concentrate on the study of the effects of the vector ordering choice on VHMT, as well as on ways of rendering the resulting operators rotation and scale invariant. Additional perspectives could include the definition of multivariate morphological operators based on the HMT, such as thinnings, thickenings and skeletons.

References

Angulo, J., 2005. Unified morphological color processing framework in a lum/sat/hue representation. In: Ronse, C., Najman, L., Decencière, E. (Eds.), Mathematical Morphology: 40 Years On. Vol. 30 of Computational Imaging and Vision. Springer-Verlag, Dordrecht, pp. 387–396.

Aptoula, E., Lefèvre, S., November 2007. A comparative study on multivariate mathematical morphology. Pattern Recognition 40 (11), 2914–2929.

Barat, C., Ducottet, C., Jourlin, M., 2003. Pattern matching using morphological probing. In: Proceedings of the 10th International Conference on Image Processing. Vol. 1. Barcelona, Spain, pp. 369–372.

Bhattacharya, P., Zhu, W., Qian, K., 1995. Shape recognition method using morphological hit-or-miss transform. Optical Engineering 34 (6), 1718–1725.

Bloomberg, D., Vincent, L., 2000. Pattern matching using the blur hit-miss transform. Journal of Electronic Imaging 9 (2), 140–150.

Doh, Y., Kim, J., Kim, J., Kim, S., Alam, M., 2002. New morphological detection algorithm based on the hit-miss transform. Optical Engineering 41 (1), 26–31.

Heijmans, H., Serra, J., 1992. Convergence, continuity and iteration in mathematical morphology. Journal of Visual Communication and Image Representation 3 (1), 84–102.

Heijmans, H. J. A. M., 1994. Morphological Image Operators. Advances in Electronics and Electron Physics Series. Academic Press, Boston.

Heijmans, H. J. A. M., Ronse, C., June 1990. The algebraic basis of mathematical morphology, part I: dilations and erosions. Computer Vision, Graphics and Image Processing 50 (3), 245–295.

Khosravi, M., Schaefer, R., 1996. Template matching based on a greyscale hit-or-miss transform. IEEE Transactions on Image Processing 5 (6), 1060–1066.

Matheron, G., 1975. Random Sets and Integral Geometry. Wiley, New York.

Naegel, B., Passat, N., Ronse, C., February 2007a. Grey-level hit-or-miss transforms - part I: Unified theory. Pattern Recognition 40 (2), 635–647.

Naegel, B., Passat, N., Ronse, C., February 2007b. Grey-level hit-or-miss transforms - part II: Applications to angiographic image processing. Pattern Recognition 40 (2), 648–658.

Raducanu, B., Grana, M., September 2000. A grayscale hit-or-miss transform based on levet sets. In: Proceedings of the 7th International Conference on Image Processing. Vol. 2. Vancouver, Canada, pp. 931–933.

Ronse, C., 1996. A lattice-theoretical morphological view on template extraction in images. Journal of Visual Communication and Image Representation 7 (3), 273–295.

Schaefer, R., Casasent, D., 1995. Nonlinear optical hit-miss transform for detection. Applied Optics 34 (20), 3869–3882.

Serra, J., 1982. Image Analysis and Mathematical Morphology Vol I. Academic Press, London.

Soille, P., March 2002a. Advances in the analysis of topographic features on discrete images. In: Proceedings of the 10th International Conference on Discrete Geometry for Computer Imagery DGCI'02. Vol. 2301 of Lecture Notes in Computer Sciences. pp. 175–186.

Soille, P., 2002b. On morphological operators based on rank filters. Pattern Recognition 35 (2), 527–535.

Soille, P., 2003. Morphological Image Analysis : Principles and Applications, 2nd Edition. Springer-Verlag, Berlin.

Weber, J., Lefèvre, S., July 2008. A multivariate hit-or-miss transform for conjoint spatial and spectral template matching. In: Proceedings of the IEEE International Conference on Image and Signal Processing. Vol. 5099 of Lecture Notes in Computer Science. Cherbourg, France, pp. 226–235.

Wilson, S., 1989. Vector morphology and iconic neural networks. IEEE Transactions on Systems, Man and Cybernetics 19 (6), 1636–1644.

Zhao, D., Daut, D., 1991. Shape recognition using morphological transformations. In: Proceedings of the 16th International Conference on Acoustics, Speech and Signal Processing. Vol. 4. Toronto, Canada, pp. 2565–2568.